PAPER

Reliable anatase-titania nanoclusters functionalized GaN sensor devices for UV assisted NO₂ gas-sensing in ppb level

To cite this article: Md Ashfaque Hossain Khan et al 2020 Nanotechnology 31 155504

View the article online for updates and enhancements.

Recent citations

- Back-Gate GaN Nanowire-Based FET Device for Enhancing Gas Selectivity at Room Temperature

 Md Ashfaque Hossain Khan et al
- Accelerated Stress Tests and Statistical Reliability Analysis of Metal-Oxide/GaN Nanostructured Sensor Devices Md Ashfaque Hossain Khan et al
- Adsorption performance of M-doped (M = Ti and Cr) gallium nitride nanosheets towards SO2 and NO2: a DFT-D calculation

Hossein Roohi and Nastaran Askari



IOP ebooks™

Bringing together innovative digital publishing with leading authors from the global scientific community.

Start exploring the collection-download the first chapter of every title for free.

IOP Publishing Nanotechnology

Nanotechnology 31 (2020) 155504 (11pp)

https://doi.org/10.1088/1361-6528/ab6685

Reliable anatase-titania nanoclusters functionalized GaN sensor devices for UV assisted NO₂ gas-sensing in ppb level

Md Ashfaque Hossain Khan^{1,3}, Brian Thomson², Ratan Debnath², Asha Rani², Abhishek Motayed² and Mulpuri V Rao^{1,3}

E-mail: mkhan53@gmu.edu and rmulpuri@gmu.edu

Received 9 October 2019, revised 26 November 2019 Accepted for publication 31 December 2019 Published 23 January 2020



Abstract

Internet of Things applications require ultra-low power, integrable into electronic circuits and mini-sized chemical sensors for automated remote air quality monitoring system. In this work, a highly sensitive and selective detection of nitrogen dioxide (NO₂) has been demonstrated by functionalizing gallium nitride (GaN) submicron wire with titania (TiO₂) nanoclusters. The twoterminal GaN/TiO₂ sensor device was fabricated by top-down approach. The photo-enabled sensing makes it possible to operate this sensor at room-temperature, resulting in a significant reduction in operating power. The GaN/TiO₂ sensor was able to detect NO₂ concentrations as low as 10 ppb in air at room temperature (20 °C) with a quick response-recovery process. The sensor was found highly selective toward NO2 against other interfering gases, such as ethanol (C₂H₅OH), ammonia (NH₃), sulfur dioxide (SO₂), methane (CH₄) and carbon dioxide (CO₂). Furthermore, principal component analysis has been performed to address the cross-sensitive nature of TiO₂. The sensor device exhibited excellent long-term stability at room temperature and humidity and was quite stable and reliable at various environmental conditions. Continuous exposure of the device to siloxane for a one-month period has shown a very small degradation in sensor response to NO₂. Finally, interaction of NO₂ gas molecules with the GaN/TiO₂ sensor has been modeled and explained under the light of energy band diagram. The photoinduced oxygen desorption and subsequent charge transfer between TiO₂ nanoclusters and NO₂ molecules modulate the depletion region width within the GaN, thus contributing to a high performance NO₂ gas sensing.

Keywords: gas sensor, titania (TiO₂), nitrogen dioxide (NO₂), selectivity, reliability, gallium nitride (GaN)

1

(Some figures may appear in colour only in the online journal)

1. Introduction

One of the six common air pollutants defined by the Environmental Protection Agency (EPA) is the highly reactive gas nitrogen dioxide (NO₂). The EPA has set short-term and long-term exposure limits for most of the known air pollutants.

EPA standards for NO₂ are 53 ppb averaged annually with a 1 h 100 ppb limit. The LC₅₀ (the lethal concentration for 50% of those exposed) for one hour of NO₂ exposure for humans has been estimated as 174 ppm [1]. The key sources of NO₂ are from combustion of fuels such as certain coals and oil [2], biomass burning due to the extreme heat of lightning during thunderstorms [3], and nitrogen fixation by microorganisms due to agricultural fertilization [4]. The notable impacts of

¹ Department of Electrical and Computer Engineering, George Mason University, Fairfax, VA 22030, United States of America

² N5 sensors, Inc., Rockville, MD 20850, United States of America

³ Authors to whom any correspondence should be addressed.

NO₂ are respiratory inflammation of the airways, decreased lung function due to long term exposure, and increased risk of respiratory conditions [5]. Moreover, it may lead to formation of fine particulate matter and ground level ozone, which have adverse health effects, and contribute to acid rain causing damage to vegetation, buildings and acidification of lakes and streams [6]. Unfortunately, individuals in need of air quality information rely on air quality data or index supplied from long distant air-monitoring stations, which makes the air quality data ineffective. Recent studies have shown that exposures to air pollutants can only be assessed accurately using time-weighted exposure measurements [7], which is only possible by using personal air quality samplers. For personal monitors to be widely accepted, the device must have the aspects such as low-cost, small size, low-power, stable operation across a wide temperature and humidity range, and long-life [8]. With prolific growth of smart devices combined with cloud-based data analytics architecture, there exists a tremendous opportunity for integrated home and personal monitoring solutions that are cost effective and efficient and can affect quality of life significantly [9]. In this respect, gas sensors can play a significant role by performing reliable detection of various toxic gases even at ppb level concentration [10, 11].

Innovativeness of this work stems from photo-enabled sensor architecture using nano-engineered semiconducting GaN micro-resistors functionalized with nanoclusters of metal-oxides [12]. Highly selective metal-oxide coating gives rise to the exceptional selectivity of these sensors [13].

Submicron/nanowires possess one-dimensional nanostructures which are particularly suited for chemical sensing due to their large surface-to-volume ratio [14]. Wide band-gap semiconductors have ability to operate at high temperatures, provide radiation and environmental stability, and mechanical robustness, which are useful for making highly selective gas sensors to operate in hostile conditions [15]. Having a direct wide band gap of 3.4 eV at room temperature, GaN is chemically very much robust. It possesses high electron mobility, high heat capacity, good thermal conductivity and high breakdown voltage which are useful properties for sensing chemical species [16]. Titanium dioxide (TiO₂) has attracted great attention due to its excellent properties such as high catalytic efficiency and wide band gap, long-term stability, low-cost and non-toxicity [17]. These characteristics make TiO₂ as one of the suitable candidates for high performance gas sensing material. Common explosives like trinitrotoluene (TNT) and other nitroaromatics detection using GaN/TiO₂ hybrid device had been demonstrated earlier by our group [18]. In this study, TiO₂ has been employed as nanocluster material on GaN submicron wire and formed by RF sputtering, utilizing enhanced surface modification technique. This nano-clustered metal-oxide layer has been found very selective to NO₂ gas molecules and facilitated high sensitivity with low detection time. The experimental details, structural characterization, electrical behavior, and gas sensing performance and mechanism of the GaN/TiO₂ sensor have been discussed in the following sections.

2. Experimental details

Schematic flow chart for the proposed device fabrication process is illustrated in figure 1. The process starts with the formation of the GaN submicron wire from the GaN wafers. This GaN wire acts as the sensor backbone. Standard RCA cleaning was performed before defining the GaN submicron pattern of width 400-500 nm by stepper lithography. Patterned metal was used as a hard mask to protect the defined GaN submicron wire during inductively coupled plasma etching. The hard mask was comprised of Ti (40 nm) and Ni (150 nm). After that, the top contact metallization was deposited on GaN in an electron beam evaporator with base pressure of 10^{-5} Pa. The deposition sequence was Ti (40 nm)/Al (80 nm)/Ti (40 nm)/Au (40 nm). A passivation layer of SiO₂ (200 nm) was added on the device by plasmaenhanced chemical vapor deposition to enhance the yield. The oxide layer over the GaN wire between the end contacts was then etched by reactive ion etching to open a window for surface functionalization. This etching was anisotropic and highly selective toward oxide. The etch rate of SiO₂ was found to be 50 nm min⁻¹, so it took 4 min to remove all the oxides. Etching was performed for an extra minute to ensure that there are no residues of oxide. The TiO2 nanoclusters were deposited on the exposed GaN submicron-wire using RF magnetron sputtering. The deposition was done in a reactive atmosphere with O₂ flow at 300 W RF power. The deposition rate was about 0.2 Å s ⁻¹ and a continuous TiO₂ layer of 5-10 nm was achieved. Lift-off was carried out with a bath of 1165 at 80 °C to pattern the metal-oxide layer. Then, rapid thermal annealing was performed with 6 slpm flow of ultrahigh purity Ar at 700 °C for 5 min to facilitate ohmic contact formation to GaN and to induce crystallization of the TiO₂ clusters. After forming thick metal bond pads with Ti (40 nm) and Au (200 nm), the fabricated sensor device was wirebonded on a 24-pin ceramic dual in line (DIP) package.

The morphology and microstructure of the fabricated TiO_2/GaN sensor were characterized by high resolution optical microscopy and field-emission scanning electron microscopy (FESEM). The elemental composition of the fabricated GaN submicron wire were verified through energy-dispersive x-ray spectroscopy. The crystallinity and phase of the sputtered TiO_2 nanoclusters were analyzed by x-ray diffraction (XRD) performed on a Bruker-AXS D8 scanning x-ray micro-diffractometer having a general area detector diffraction system using $Cu-K\alpha$ radiation. The surface morphology and roughness of the TiO_2/GaN sensor were obtained with atomic force microscopy (AFM) using a Bruker Dimension FastScan system.

The current–voltage (*I–V*) and photocurrent measurements of the fabricated sensor were performed by a National Instrument PCI DAQ system. UV illumination to the sensor was applied by a 365 nm light emitting diode. The output power of the UV source was maintained at 470 mW cm⁻² with less than 0.4% variation, as verified with a Newport power meter. For gas sensing measurements the device was placed in a custom designed gas chamber made of stainless steel. A gaseous mixture of NO₂ and compressed breathing

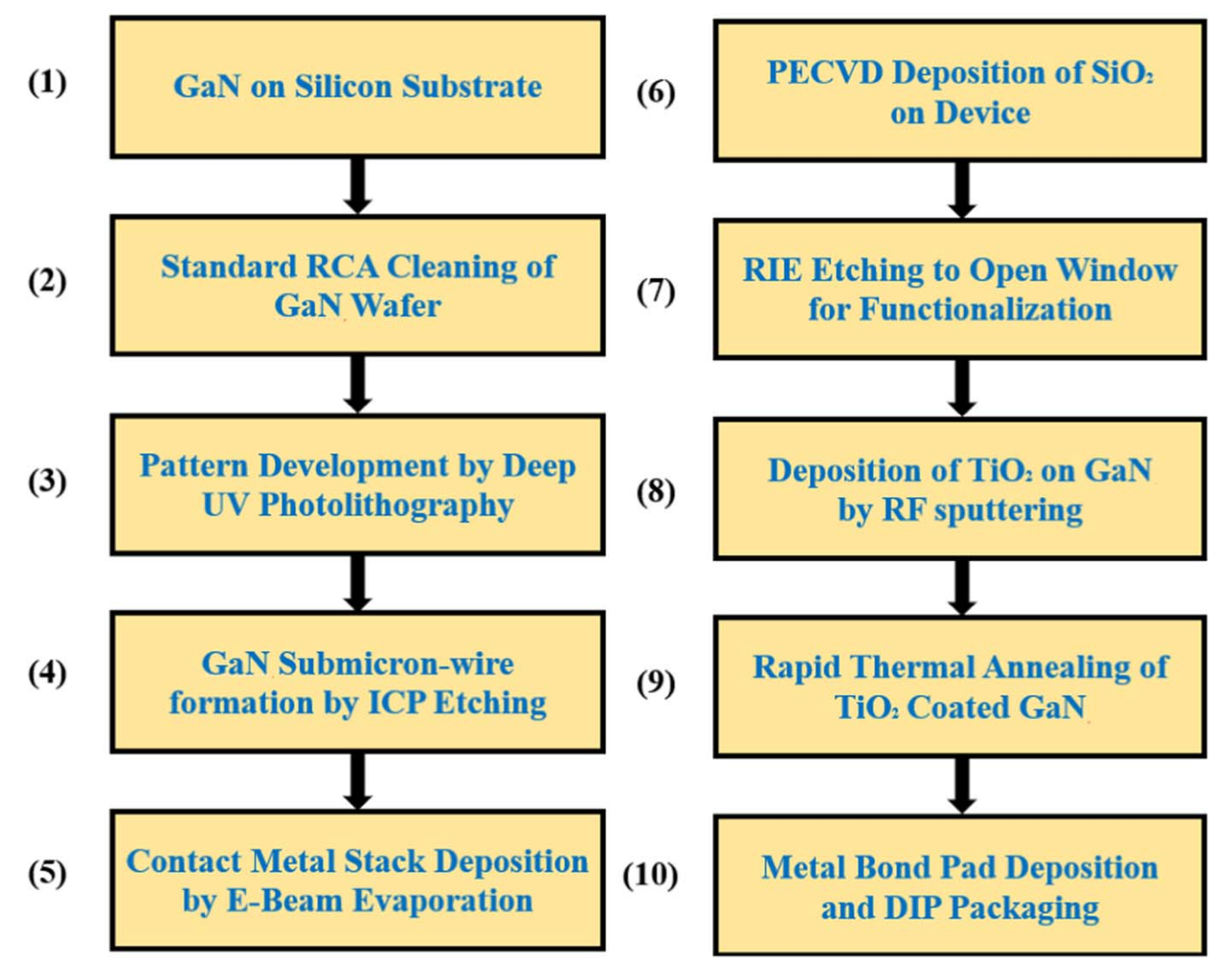


Figure 1. Schematic flow chart for the proposed sensor fabrication process.

air was introduced into the sensing apparatus and the net flow (air + NO₂) was maintained at 100 sccm. Mass flow controllers independently controlled the flow rate of each component, determining the composition of the mixed gas. The devices were biased with a constant 5 V supply and currents were measured by a National Instrument PCI DAQ system. After the sensor was exposed to NO2, it had been allowed to regain the baseline current with the air-analyte gas turned off, without purging the gas chamber. Sensor response has been determined as $(R_{gas}-R_{air})/R_{air}$, where R_{gas} and R_{air} are the resistances of the sensor in the presence of the analyte-air mixture and in the presence of air, respectively. Bronkhorst controlled evaporator and mixer has been used as the core component for environmental humidity generation and control. Device reliability tests at different environmental conditions were performed in a Tenny BTRC temperature and humidity test chamber. It is set conditions are controlled by a bidirectional PID controller with resolution of 0.1 °C and 1% relative humidity, respectively.

3. Results and discussion

3.1. Morphological and structural characterization

The actual optical image of the proposed TiO₂/GaN sensor device is displayed in figure 2(A). It is a lightly doped $0.4-0.5 \mu m$ wide GaN micro-resistor structure developed on silicon substrate and functionalized with a continuous layer of photocatalytic metal-oxide. Figure 2(B) shows FESEM image of a typical device with a TiO₂ coated GaN submicron-wire positioned between the two metal electrodes. The size of the submicron-wire sample is observed quite uniform having a height and width of 400 nm and 400-500 nm respectively. Since TiO₂ deposited GaN is very small in size, a reference sample with TiO₂ thin film (30 nm) on sapphire substrate was prepared to detect the XRD signals and AFM images. The thin film was made with almost similar thickness and was annealed at the same condition, expecting that similar TiO₂ morphology has been formed on the substrate as in the TiO2 coated GaN case. The XRD pattern of annealed TiO2 thin film is presented in figure 3(A). The major diffraction peaks are exhibited at 25.42°, 48.1°, 53.7°, and 55.6°, which are

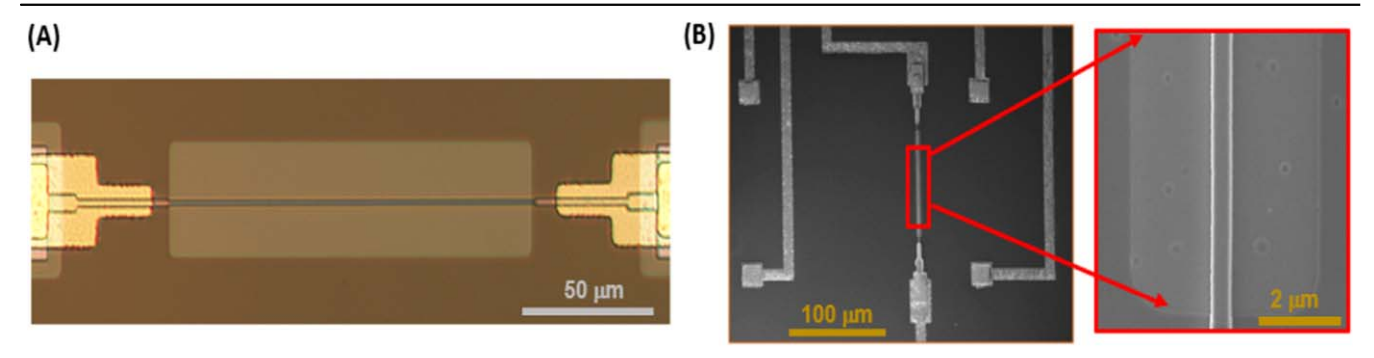


Figure 2. (A) The optical image showing the top view of the fabricated TiO₂/GaN sensor. (B) FESEM image of the TiO₂/GaN sensor device. Magnified image shows top view of the GaN submicron-wire.

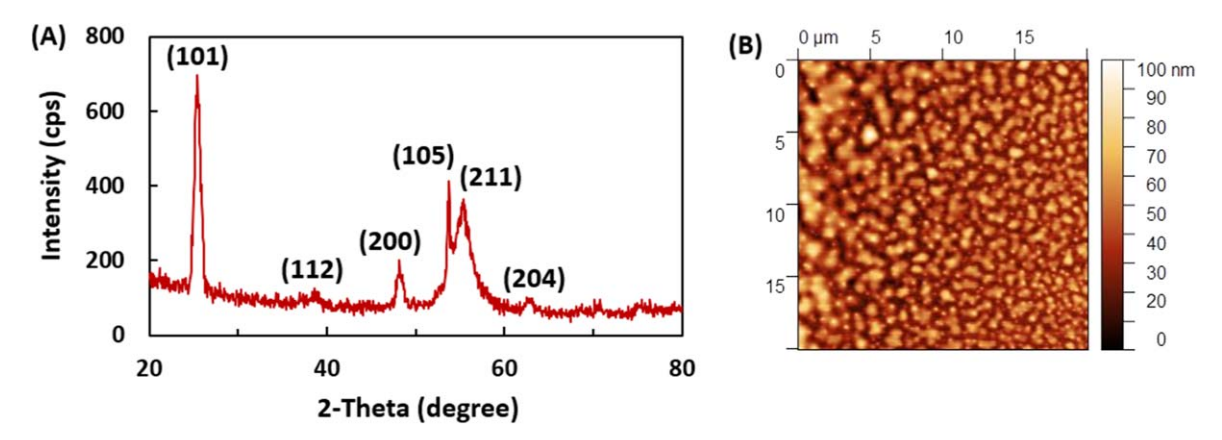


Figure 3. (A) X-ray diffraction pattern of TiO₂ thin film. (B) The two-dimensional atomic force microscopy (AFM) image of TiO₂ thin film.

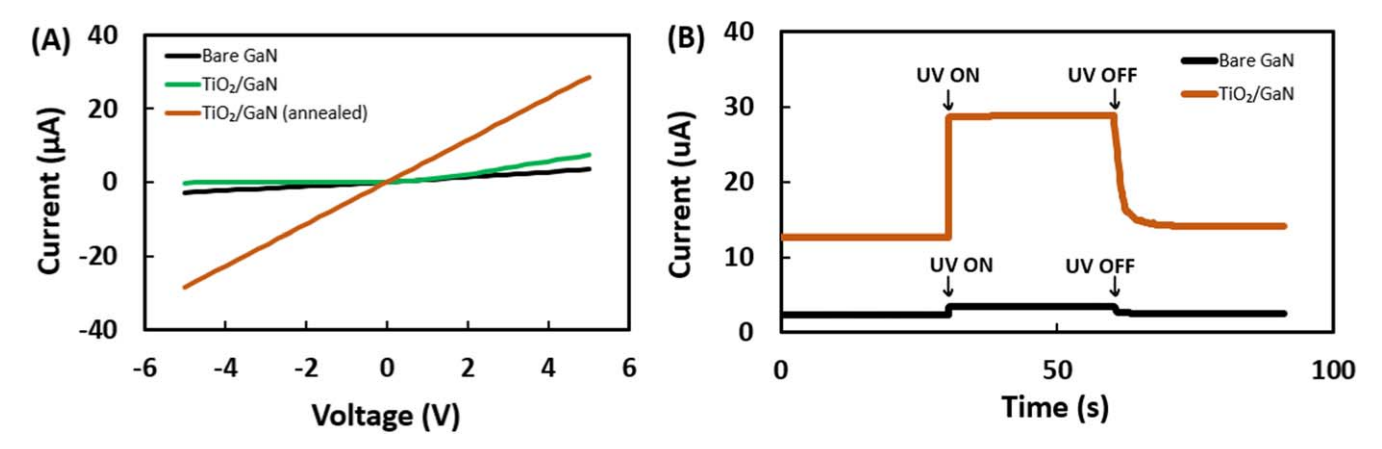


Figure 4. (A) I-V characteristics of a GaN two-terminal device under UV light at different stages of fabrication. (B) Dynamic photocurrent of a bare GaN and TiO₂-coated GaN device at room temperature (20 °C) with an applied voltage of 5 V.

attributed to the planes (101), (200), (105) and (211) of anatase TiO_2 .

The two-dimensional AFM image of TiO_2 film is shown in figure 3(B) which reveals the advanced surface morphologies of the sputtered oxide. The root mean square surface roughness of TiO_2 was found to be 20.1 nm. This moderate surface roughness of the deposited metal oxide facilitates a larger gas sensing response than that of highly uniform surface. Ohmic contacts have been formed between the electrodes and the submicron-wire. The contact resistance has been calculated as 190 k Ω approximately.

3.2. Current–voltage (I–V) characterization

The fabricated GaN submicron-wire is a two-terminal device whose I–V characteristics are shown in figure 4(A). It is clearly seen that current response of the bare submicron-wire was nonlinear and asymmetric. With the incorporation of TiO_2 nanoclusters on bare GaN, current magnitude got increased. This happens due to reduction of surface depletion within the submicron-wire introduced by adsorbed oxygen molecules [19]. After annealing the device at 700 °C for 300 s, the I–V response became linear with enhanced current magnitude. This indicates the formation of low resistance

ohmic contacts to the GaN [20]. Besides, UV illumination contributed in the enhancement of sensor current magnitude and linearity. This is attributed to the fact that upon UV excitation, the metal oxide photo-desorbs water and oxygen creating surface defect active sites and thus electron—hole pairs are generated in the GaN backbone.

Figure 4(B) shows the dynamic photocurrent of a bare GaN device and the TiO₂-deposited GaN device, when exposed to UV light with an applied voltage of 5 V. The GaN/TiO₂ device exhibited almost two orders of increase in current magnitude when exposed to UV light as compared to the similar-diameter bare device. This improvement is due to the separation of photogenerated charge carriers by a surface depletion field, thereby increasing the lifetime of the photocurrent decays rapidly but cannot return to the dark current value. This can be explained by the phenomenon of sustained photoconductivity of the submicron/nanowire [21].

3.3. Gas sensing behavior

In order to evaluate the sensing performance of the fabricated device, response of the sample to NO2 gas with different concentrations was measured at room temperature (20 °C). The bare GaN device did not respond well to the target gas even for high concentrations. In contrast, GaN/TiO₂ device exhibited significant change in the photocurrent when exposed to NO2 gas in the presence of UV light. The device current recorded with 100 sccm of air flowing though the sensing chamber under UV illumination was established as a reference for our experiments. As shown in figure 5(A), the dynamic photocurrent response of the TiO2 coated GaN sensor decreases quickly and rises rapidly when varying concentrations of NO₂ from 1 ppb to 500 ppm in dry air are introduced consecutively into and removed from the testing atmosphere. When gas flow was turned off, the sensor had been allowed to recover at room temperature without any additional purging. The sensor showed a maximum response of 32% on exposure to 500 ppm NO₂ with a lowest detection limit of 1 ppb. Though the sensor did not respond well at dark condition, sensor photocurrent decreased significantly in comparison to dry air response under UV light.

The normalized responses of the TiO_2/GaN sensor with and without UV light are plotted as a function of NO_2 gas concentration in figure 5(B). The fitting equations of the sensor response Y and gas concentration X are stated as $Y = 2.43 \ln X + 15.44$ and $Y = 0.825 \ln X + 5.39$ in presence and absence of UV light, respectively, and the regression coefficients are 0.9446 and 0.9176, respectively. The higher magnitude curve with steeper slope under UV illumination indicates the contribution of UV light to the enhancement of the gas sensing response.

It is well known that response and recovery times are important parameters for evaluating gas sensing performance of sensors. Response time is defined as the time to reach 90% of the final value during NO₂ exposure. Recovery time is similarly defined as the time to reach 90% of the final value during clean air exposure. Response and recovery times of the

sensor were obtained for all the measured responses at different concentrations as plotted in figure 6(A). It was found that, response time kept decreasing initially with the increase of NO_2 concentration and become nearly constant at higher gas concentrations. The faster response at higher gas concentration is attributed to the rise of diffusion rate of gas molecules with the increase of concentration. Also, recovery process got slower than the corresponding response process with the increasing NO_2 concentration.

In order to test long term stability, the sensor response was collected continuously for 20 d at high and low gas concentrations as presented in figure 6(B). It has been observed that gas response of the sensor was almost constant over time, particularly for high concentration. The response change at low concentration was very little as well. Degradation of gas response over 20 d were 1.9%, 1.3% and 0.4% for 10 ppb, 1 ppm and 500 ppm of NO₂ gas, respectively. Since sensor response to 1 ppb of NO₂ showed some degradation over long period, we set 10 ppb as the lowest limit of detection for the TiO₂/GaN sensor device.

To ensure applicability in practical environment, especially in industrial arena, selectivity of the sensor is very important. The selectivity was studied by exposing the proposed sensor to various interfering gases including ethanol (C₂H₅OH), ammonia (NH₃), sulfur dioxide (SO₂), methane (CH₄), and carbon dioxide (CO₂). Figure 6(C) illustrates the comparative percent response histograms for TiO₂/GaN sensor toward three different level of concentrations of these target gases at room temperature under dry air. Clearly, the response toward NO2 is much higher than that of other test gases which demonstrates the selective feature of our sensor. Furthermore, the sensor showed moderate response toward ethanol at high concentration which can contribute minor cross-sensitivity to NO₂ responses if present in the background. We can resolve this issue by applying principal component analysis (PCA) technique on the experimental gas response data.

Gas response outcome, such as response magnitude, response time and recovery time were used as input parameters in PCA analyses. For the two test gases (NO₂ and ethanol), we collected gas responses for 5 different concentrations, and repeated the measurements 3 times. The input dataset was a 30×3 matrix in which 60% had been used as training set and 40% as test set. A threshold variance of 99% was set during component analysis. Figure 6(D) shows the PC_2 versus PC_1 plot comprising 98% of the total variance which clearly differentiate between NO₂ gas and ethanol vapor. All the raw data processing and PCA-analysis had been performed in the RapidMiner studio software.

Device reliability is an important attribute to consider in case of practical applicability of sensor devices. The proposed GaN/TiO₂ based sensor was tested at various environmental humidity and temperature conditions for 1 ppm of NO₂ exposure, as shown in figure 7(A). It was observed that sensor response was slightly enhanced with increasing humidity and got almost constant at high humid conditions. This happens because water molecules give away electrons on the sensor surface and neutralize the photo-generated holes within the

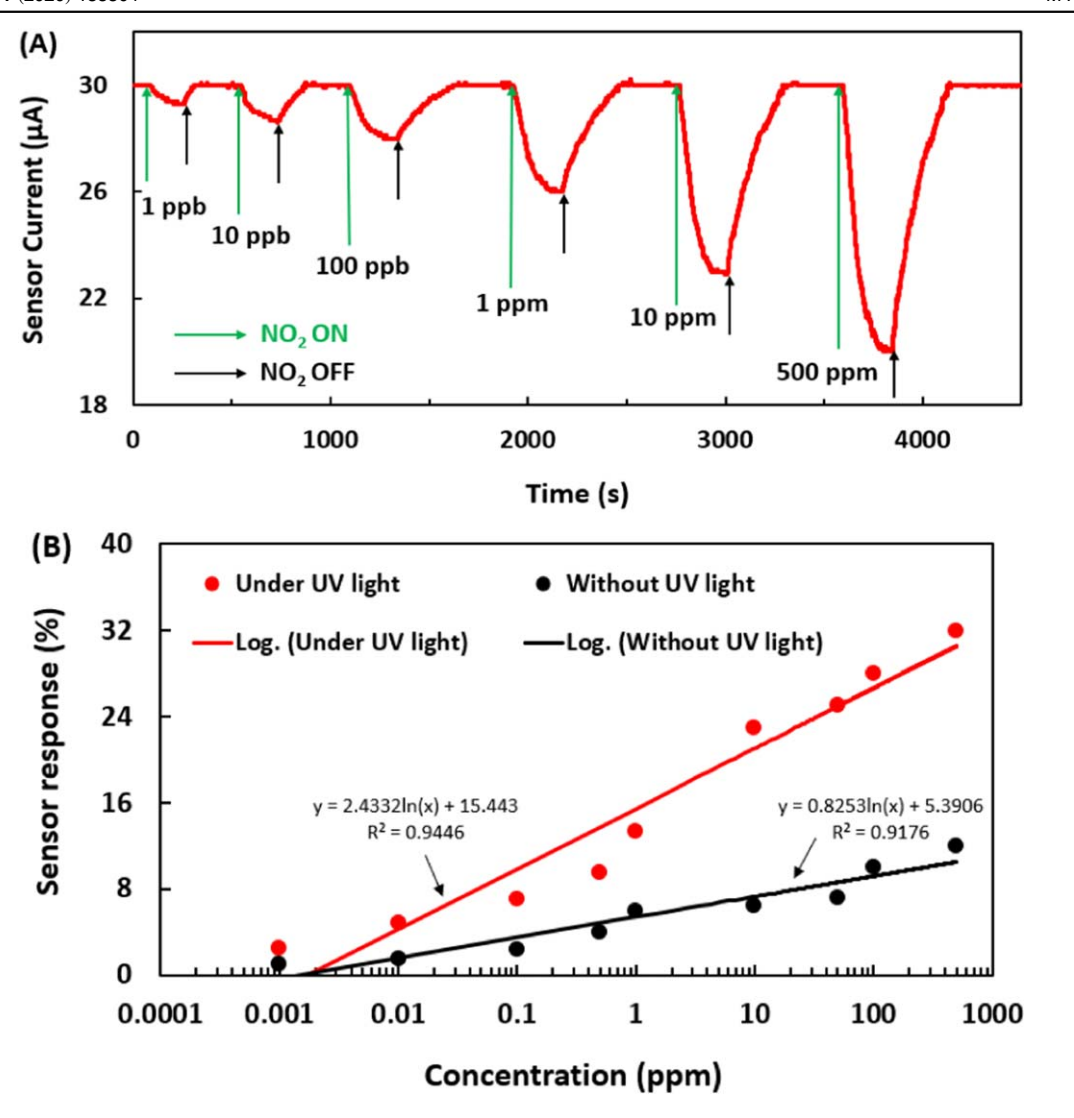


Figure 5. (A) Sensor current responses, and (B) function fitting curves of the of GaN/TiO₂ sensor to varying concentrations of NO₂ gas ranging from 1 ppb to 500 ppm in dry air under UV light and without UV light at room temperature (20 °C).

sensor. With the increasing humidity (water molecules), more holes are neutralized and thus leave more electrons to be used for NO₂ molecules adsorption which leads to the rise of depletion region within the sensor. This phenomenon explains the fact of lowering the steady-state resistance and increasing senor resistance response with the increasing humidity. Also, a diminishing response increase was seen at higher operating temperatures. Therefore, the proposed sensor device exhibited reliable and stable performance at various environmental situations avoiding any significant response deviations.

Now-a-days, silicon-containing compounds are found in numerous products. Particularly, metal-oxide based gas sensors encounter poor long-term stability even at low concentrations of siloxanes present in atmosphere [22]. Accelerated siloxane stability test has been performed on our NO₂ sensor devices in the presence of Decamethylcyclopentasiloxane (D5). The sensor device was exposed to 200 ppm of D5 siloxane for one month. 1 ppm NO₂ gas response data was taken at different intervals within that time period. It is found that there is only a small

degradation in response over one month as illustrated in figure 7(B). The robustness of the sensor response against the siloxane is mainly attributed to the UV light which is used during NO_2 gas detection. Due to long term exposure, siloxane molecules are adsorbed on the sensor surface and a layer is formed. UV illumination helps to desorb those molecules and cleans-up the metal oxide surface for NO_2 molecules adsorption. A continuous UV exposure, even during the absence of exposure to NO_2 , may result in a very negligible effect of siloxanes on the response of the device to the NO_2 gas. Thus, the responses of the device remain almost unaffected to the siloxanes.

Table 1 summarizes the comparison of nitrogen dioxide sensing performance of GaN/TiO₂ sensor device with other recently reported NO₂ sensor devices. For a gas sensor to be widely accepted it must have high response, quick response-recovery, precise selectivity, long operating life and stable operation across various environmental conditions. No such gas sensor has been reported yet having all these desired properties. For instance- some reported sensors may exhibit

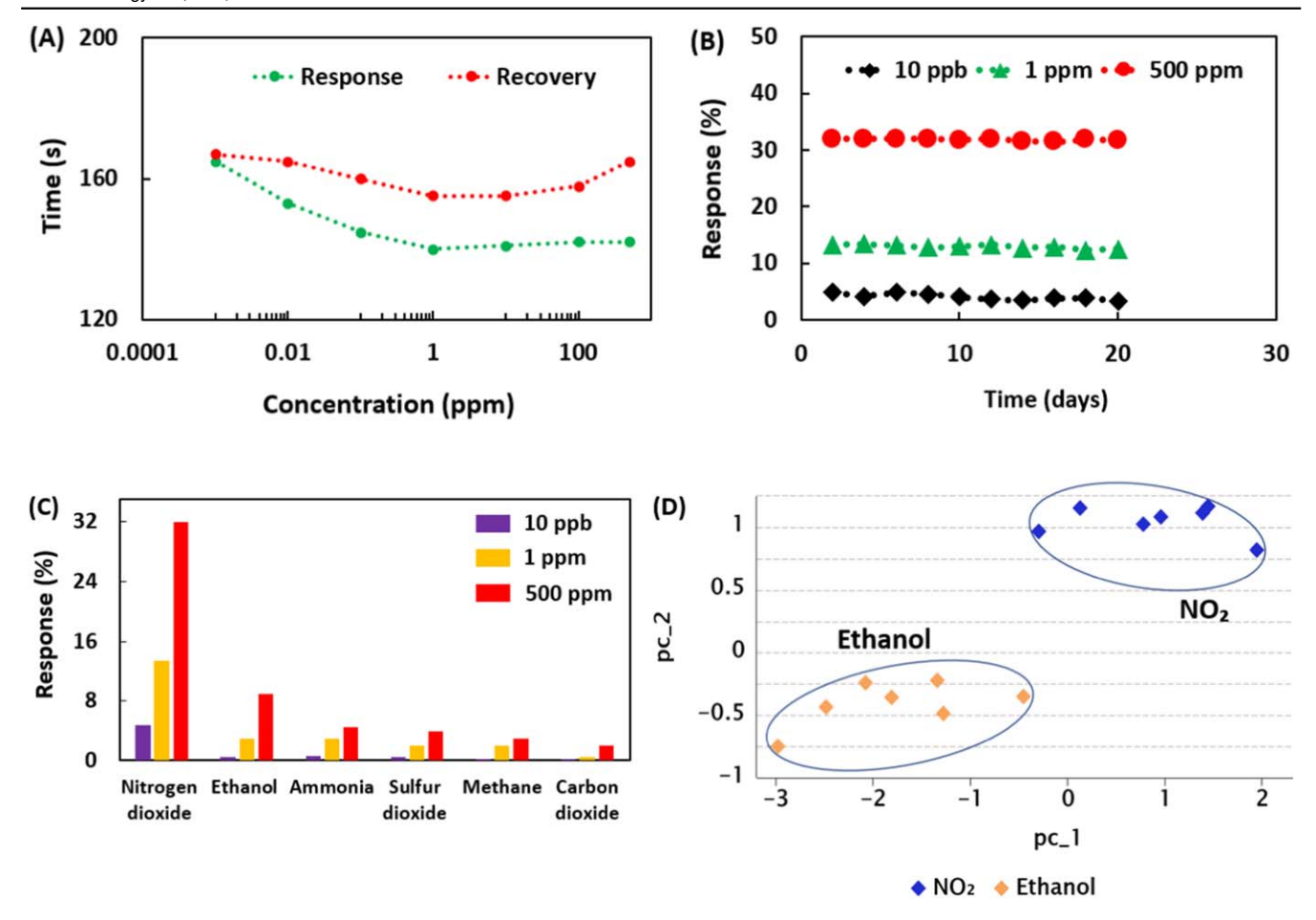


Figure 6. (A) Response/recovery times of the sensor obtained at various NO_2 concentrations ranging from 1 ppb to 500 ppm at room temperature. (B) Long-term stability of the sensor tested at 10 ppb, 1 ppm and 500 ppm of NO_2 gas. (C) Cross-sensitivity test for TiO_2/GaN sensor to various background gases at test concentrations of 10 ppb, 1 ppm and 500 ppm of each gas. (D) Principal component analysis: PC_2 versus PC_1 plot for 6 different concentrations of NO_2 gas and ethanol vapors exposed to the sensor, which includes up to 98% of the total variance.

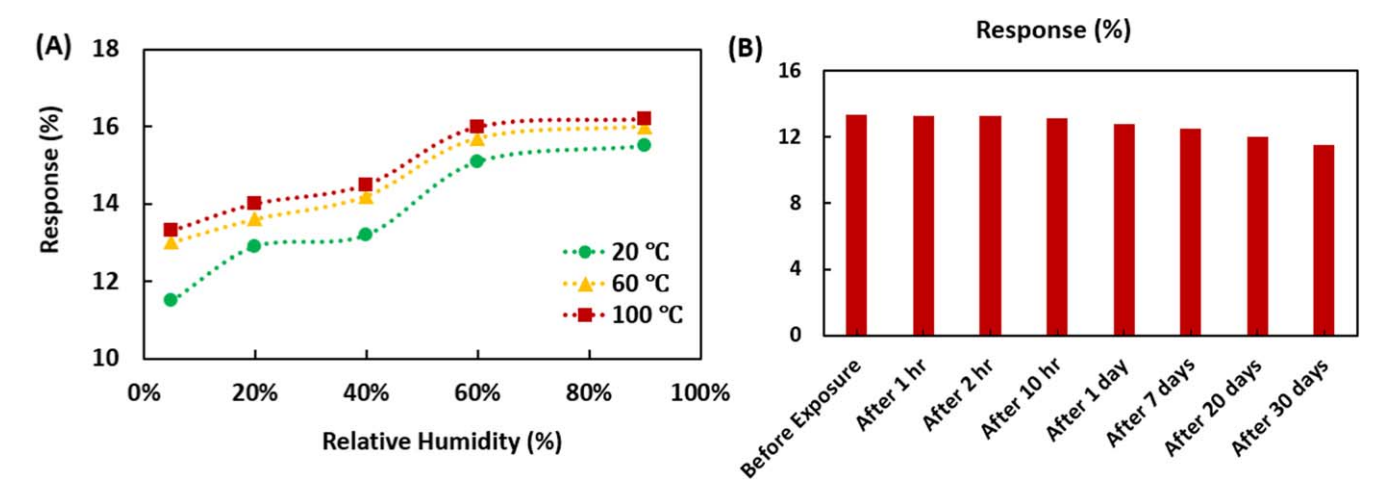


Figure 7. (A) Responses of GaN/TiO₂ sensor at various environmental humidity and temperature conditions for 1 ppm of NO₂ exposure. (B) Accelerated siloxane stability test results in terms of 1 ppm NO₂ responses over one-month time period at room temperature (20 °C).

very high response, but their response-recovery processes are slow. Some of them are good in many respects but not adaptive to change of environmental conditions. Furthermore, the sensors which have those desired properties are not compatible for low-cost large-scale production. Our gas sensor was made using top-down fabrication method along with optimized and well controlled process steps, which make it feasible for large scale production. Also, UV assisted gas

Table 1. Comparison of nitrogen dioxide sensing performance of TiO₂/GaN sensor with other recently reported NO₂ sensors.

Materials	Structure	Operating temperature (°C)	Concentration (ppm)	Sensitivity/ response	Response time (s)	Recovery time (s)
GaN/TiO ₂ (this work)	Submicron wire- Nanocluster	RT	1	13.33	140	160
SnO ₂ /NRGO [24]	Nanosheets	RT	5	1.38	45	168
Graphene–SnO ₂ [25]	Nanocomposites	150	1	24.7	175	148
SnO ₂ /graphene [26]	Nanocomposites	RT	5	171	7 min	Long
RGO-polythiophene [27]	Thin film	RT	10	26.36	<180	< 200
Ion-beam irradiated SnO ₂ [28]	Nanowire	150	2	14.2	292	228
MoS ₂ [29]	Flakes	RT (UV)	100	27.92	29	350
Hierarchical ZnO–RGO [30]	Nanosheets	100	0.05	12	306	450
MoS ₂ /graphene [31]	Aerogel	200	0.5	9.1	21.6	29.4
2, 2 1 1 3	Ü	(microheater)				
SnO ₂ -polyaniline [32]	Heterostructure thin film	25	50 ppb	5%	5 min	15 min
RGO/poly(3,4-ethylenediox-ythiophene) [33]	Nanocomposite	RT	1	0.05	<180	< 70
RGO/Au [34]	Nanocomposite	50	5	1.33	132	386
Mixed p type MoS ₂ [35]	Flakes	RT+UV	10	21.78	6.09	146.49
MoS ₂ [36]	Nanowire networks	60	5	18.1	16	172
Nb doped-MoSe ₂ [37]	2D Layered	150	3	8.03	< 30	
PS/WO ₃ -Pd60 [38]	Nanorods	RT	2	5.2	10	339
Polycrystalline PdO [39]	Ultrathin films	175	10	1.63	< 500	600-700
ZnO [40]	Nanorods	200	100	622	35	206
Microwave-synthesized NiO [41]	Film	25	3	4991	30	45
Pt-AlGaN/GaN [42]	HEMT	300	900	33	27 min	_
PCDTBT [43]	OFET	RT	10	160	6.5 min	33 min
Copper phthalocyanine	Thin film	RT	20	>550	_	>3 days
(CuPc) [44]	transistor					j
MoS ₂ –RGO [45]	Nanosheets	160	3	1.23	8	20
ZnO/poly(3-hex- ylthiophene) [46]	Nanosheet- nanorod	RT	4	59	<15 min	<45 min

sensing consumes less power than microheater or external heating assisted sensing to achieve full sensor recovery [23]. Being adequately sensitive to the target gas with a reasonable response-recovery time, the GaN/TiO₂ sensor exhibits stable operation across a wide temperature and humidity range. It has the advantages of ultra-low power operation, low-cost, ultra-small size and weight, radiation-tolerance, long-operating life, non-heat producing and non-toxic which make this gas sensor suitable for the integration in embedded-chip or plug-in module.

4. Gas sensing mechanism

Sensing of NO₂ molecules using the metal oxide nanoclusters functionalized GaN sensor can be understood using the simplified schematic in figure 8(A). The basic sensing mechanism can be explained as: (1) upon UV illumination the metal-oxide nanocluster photo-desorbs water and oxygen creating surface defect active sites and electron-hole pairs are generated in the GaN backbone; (2) target analytes chemisorb

at those active sites; (3) dynamic trapping and de-trapping of charge carriers at those active sites by the adsorbed molecules causes surface potential modification of the GaN backbone, leading to (4) modulation of the sensor current, which is proportional to the analyte concentration.

Oxygen molecules are chemisorbed in the Ti³⁺ vacancy sites on the TiO₂ surface acquiring a negative charge [47]. Also, water molecules undergo molecular or dissociative adsorption on the TiO2 cluster surface creating OH- species on the Ti³⁺ defect sites [48]. It is well known that surface depletion amount within GaN governs its dark conductivity. Under UV excitation with an energy above the bandgap energy of GaN (3.4 eV) and TiO₂ (3.2 eV), electron-hole pairs are produced both in the GaN and in the TiO2 cluster. Since photogenerated holes diffuse toward the GaN surface due to the surface band bending, carrier lifetime and thus the photocurrent increases within GaN submicron-wire. On the other hand, the chemisorbed oxygen and water molecules on TiO₂ nanoclusters receive the photogenerated holes and get desorbed. NO₂ molecules are directly adsorbed onto these freshly produced sites due to their high electrophilic property.

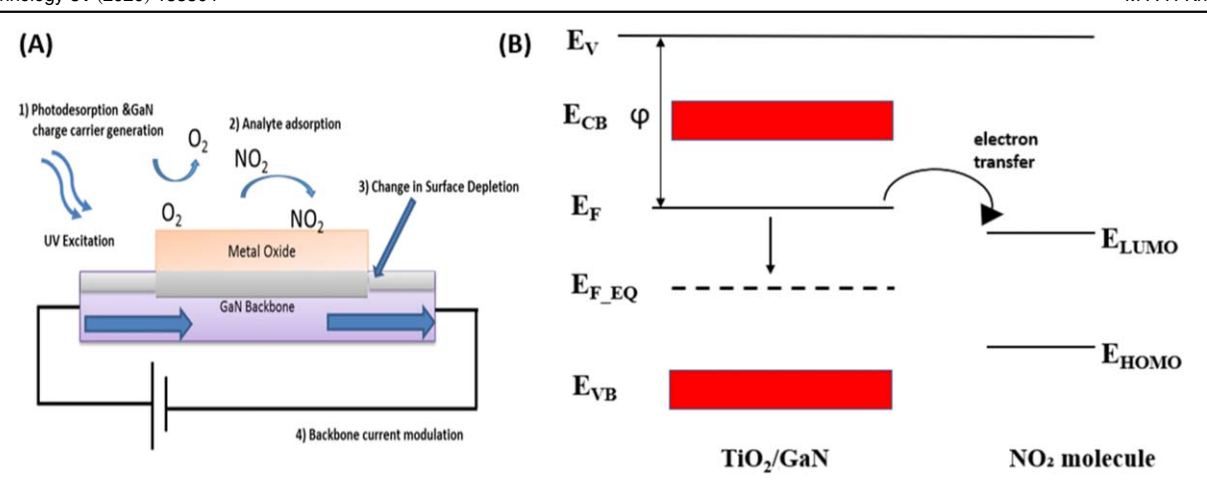


Figure 8. (A) Gas sensing mechanism illustration using schematic representation of the GaN (submicron-wire)– TiO_2 (layer of metal oxide nanoclusters) sensor (not to scale) to NO_2 analyte in presence of UV excitation. (B) Charge transfer mechanism of TiO_2/GaN and NO_2 molecule within the energy band diagram. Here, ϕ , E_V , E_F and $E_{F,EQ}$ represent work function of the TiO_2/GaN , energy of vacuum level, Fermi energy of the TiO_2/GaN , and the equilibrium state of the adsorption system, respectively. E_{CB} and E_{VB} denote conduction and valence band, respectively. E_{LUMO} and E_{HOMO} indicate the orbital energies of NO_2 molecule.

Some NO_2 molecules interact with the chemisorbed oxygen species on the surface and get adsorbed thereby. This charge transfer between the TiO_2 nanoclusters and the NO_2 molecules raises the depletion region width within the GaN, thus decreases the sensor current. In this way, the device response is modulated with the depletion region alteration caused by the change in NO_2 gas concentration.

Figure 8(B) shows the charge transfer mechanism of ${\rm TiO_2/GaN}$ and ${\rm NO_2}$ molecule under the light of energy band diagram. When energy gap from Fermi energy to LUMO of gas molecule is much less than that of HOMO of gas molecule, ${\rm TiO_2}$ electrons prefer to move toward the LUMO of the ${\rm NO_2}$ molecule by quantum tunneling. In consequence, Fermi energy of the ${\rm TiO_2/GaN}$ device begins to move toward valence band region. This charge transfer process comes to an end when an equilibrium Fermi energy ($E_{\rm F_EQ}$) is established between the device and gas molecules.

5. Future perspectives and conclusion

In this paper, we demonstrated highly selective and sensitive NO2 gas sensor using GaN submicron-wire decorated with TiO₂ nanoclusters. The GaN/TiO₂ sensor was able to detect NO₂ concentration as low as 10 ppb in air at room temperature with reasonable response-recovery process. The sensor showed high stability and excellent reproducibility toward the analyte gas exposures. The nanoengineered surface modification applied here is unique compared to traditional commercially available metal oxide sensors, as those need to be heated to remove the stable adsorbed oxygen and water from the defect sites, resulting in high-power requirement. The nano photo-catalyst can be activated using low-power UV LEDs, leading to significant reduction in operating power. Due to the use of inert wide-bandgap semiconductor and metal oxide, the environmental impact of our sensors during their life cycles is minimal. Future applications of such low-power, robust and small form-factor sensors include embedded-chip or plug-in module with multi-analyte sensor arrays for the smart phones for citizens and soldiers for acquiring real-time environmental information.

Acknowledgments

This work was supported by the NSF grant# ECCS1840712. The GaN/TiO₂ submicron-wire based NO₂ gas sensing devices were fabricated in the Nanofab of the NIST Center for Nanoscale Science and Technology. Gas sensing measurements were conducted at N5 Sensors, Inc.

Conflicts of interest

The authors declare no conflict of interest. The funders had no role in the design of the study; in the collection, analyses, or interpretation of data; in the writing of the manuscript, or in the decision to publish the results.

ORCID iDs

Md Ashfaque Hossain Khan https://orcid.org/0000-0002-0070-8872

References

[1]
National Research Council Subcommittee on Rocket-Emission Toxicants 1998 Acute toxicity of nitrogen dioxide Assessment of Exposure-response Functions for Rocketemission Toxicants (Washington DC: National Academies Press) https://ncbi.nlm.nih.gov/books/NBK230446/

- [2] Anenberg S C et al 2017 Impacts and mitigation of excess diesel-related NO_x emissions in 11 major vehicle markets Nature 545 467–71
- [3] Boleij J S M et al 1967 Domestic air pollution from biomass burning in Kenya Atmos. Environ. 23 1677–81
- [4] Robinson E and Robbins R C 1970 Gaseous nitrogen compound pollutants from urban and natural sources J. Air Pollut. Control Assoc. 20 303–6
- [5] Ehrlich R 1966 Effect of nitrogen dioxide on resistance to respiratory infection *Bacteriol. Rev.* 30 604–14
- [6] Genc S, Zadeoglulari Z, Fuss S H and Genc K 2012 The adverse effects of air pollution on the nervous system J. Toxicol. 2012 1–23
- [7] Henderson R 2013 Lower limits lead to conservative sensor settings *Industrial Safety & Hygiene News* https://ishn. com/articles/95851-lower-limits-lead-to-conservativesensor-settings
- [8] Lin C et al 2018 High performance colorimetric carbon monoxide sensor for continuous personal exposure monitoring ACS Sens. 3 327–33
- [9] Suh J-H et al 2018 Fully integrated and portable semiconductor-type multi-gas sensing module for IoT applications Sens. Actuators B 265 660–7
- [10] Khan M, Rao M and Li Q 2019 Recent advances in electrochemical sensors for detecting toxic gases: NO₂, SO₂ and H₂S Sensors 19 905
- [11] Rani A, DiCamillo K, Khan M A H, Paranjape M and Zaghloul M E 2019 Tuning the polarity of MoTe₂ FETs by Varying the channel thickness for gas-sensing applications Sensors 19 2551
- [12] Aluri G S et al 2011 Highly selective GaN-nanowire/TiO₂-nanocluster hybrid sensors for detection of benzene and related environment pollutants Nanotechnology 22 295503
- [13] Aluri G S *et al* 2012 Methanol, ethanol and hydrogen sensing using metal oxide and metal (TiO₂–Pt) composite nanoclusters on GaN nanowires: a new route towards tailoring the selectivity of nanowire/nanocluster chemical sensors *Nanotechnology* **23** 175501
- [14] Wang Z L 2006 Novel nanostructures and nanodevices of ZnO Zinc Oxide Bulk, Thin Films and Nanostructures (Amsterdam: Elsevier) pp 339–70
- [15] Tsao J Y et al 2018 Ultrawide-bandgap semiconductors: research opportunities and challenges Adv. Electron. Mater. 4 1600501
- [16] Nahhas A M 2018 Review of GaN nanostructured based devices AJN 6 1–14
- [17] Fujishima A and Honda K 1972 Electrochemical photolysis of water at a semiconductor electrode *Nature* 238 37–8
- [18] Aluri G S, Motayed A, Davydov A V, Oleshko V P, Bertness K A and Rao M V 2013 Nitro-aromatic explosive sensing using GaN nanowire-titania nanocluster hybrids *IEEE Sensors J.* 13 1883–8
- [19] Zywietz T K, Neugebauer J and Scheffler M 1999 The adsorption of oxygen at GaN surfaces Appl. Phys. Lett. 74 1695–7
- [20] Motayed A, Bathe R, Wood M C, Diouf O S, Vispute R D and Mohammad S N 2003 Electrical, thermal, and microstructural characteristics of Ti/Al/Ti/Au multilayer Ohmic contacts to n-type GaN J. Appl. Phys. 93 1087–94
- [21] Sanford N A et al 2010 Steady-state and transient photoconductivity in c-axis GaN nanowires grown by nitrogen-plasma-assisted molecular beam epitaxy J. Appl. Phys. 107 034318
- [22] Rüffer D, Hoehne F and Bühler J 2018 New digital metaloxide (MO_x) sensor platform Sensors 18 1052
- [23] Wu J, Tao K, Miao J and Norford L K 2015 Improved selectivity and sensitivity of gas sensing using a 3D reduced

- graphene oxide hydrogel with an integrated microheater ACS Appl. Mater. Interfaces 7 27502–10
- [24] Wang Z et al 2017 High-performance reduced graphene oxide-based room-temperature NO₂ sensors: a combined surface modification of SnO₂ nanoparticles and nitrogen doping approach Sens. Actuators B 242 269–79
- [25] Kim H W et al 2017 Microwave-assisted synthesis of graphene–SnO₂ nanocomposites and their applications in gas sensors ACS Appl. Mater. Interfaces 9 31667–82
- [26] Tammanoon N et al 2015 Ultrasensitive NO₂ sensor based on ohmic metal–semiconductor interfaces of electrolytically exfoliated graphene/flame-spray-made SnO₂ nanoparticles composite operating at low temperatures ACS Appl. Mater. Interfaces 7 24338–52
- [27] Bai S *et al* 2016 Enhancement of NO₂ -sensing performance at room temperature by graphene-modified polythiophene *Ind. Eng. Chem. Res.* **55** 5788–94
- [28] Kwon Y J, Kang S Y, Wu P, Peng Y, Kim S S and Kim H W 2016 Selective improvement of NO₂ gas sensing behavior in SnO₂ nanowires by ion-beam irradiation ACS Appl. Mater. Interfaces 8 13646–58
- [29] Kumar R, Goel N and Kumar M 2017 UV-activated MoS₂ based fast and reversible NO₂ sensor at room temperature ACS Sens. 2 1744–52
- [30] Liu J et al 2017 Ultrasensitive and low detection limit of nitrogen dioxide gas sensor based on flower-like ZnO hierarchical nanostructure modified by reduced graphene oxide Sens. Actuators B 249 715–24
- [31] Long H et al 2016 High surface area MoS₂/graphene hybrid aerogel for ultrasensitive NO₂ detection Adv. Funct. Mater. 26 5158–65
- [32] Betty C A, Choudhury S and Arora S 2015 Tin oxide polyaniline heterostructure sensors for highly sensitive and selective detection of toxic gases at room temperature Sens. Actuators B 220 288–94
- [33] Yang Y, Li S, Yang W, Yuan W, Xu J and Jiang Y 2014 In situ polymerization deposition of porous conducting polymer on reduced graphene oxide for gas sensor ACS Appl. Mater. Interfaces 6 13807–14
- [34] Zhang H, Li Q, Huang J, Du Y and Ruan S C 2016 Reduced graphene oxide/Au nanocomposite for NO₂ sensing at low operating temperature *Sensors* 16 1152
- [35] Agrawal A V et al 2018 Photoactivated mixed in-plane and edge-enriched p-type MoS₂ flake-based NO₂ sensor working at room temperature ACS Sens. 3 998–1004
- [36] Kumar R, Goel N and Kumar M 2018 High performance NO₂ sensor using MoS₂ nanowires network Appl. Phys. Lett. 112 053502
- [37] Choi S Y et al 2017 Effect of Nb doping on chemical sensing performance of two-dimensional layered MoSe₂ ACS Appl. Mater. Interfaces 9 3817–23
- [38] Qiang X et al 2018 Effect of the functionalization of porous silicon/WO₃ nanorods with Pd nanoparticles and their enhanced NO₂-sensing performance at room temperature Materials 11 764
- [39] Ievlev V M, Ryabtsev S V, Samoylov A M, Shaposhnik A V, Kuschev S B and Sinelnikov A A 2018 Thin and ultrathin films of palladium oxide for oxidizing gases detection *Sens*. *Actuators* B 255 1335–42
- [40] Navale Y H et al 2017 Zinc oxide hierarchical nanostructures as potential NO₂ sensors Sens. Actuators B 251 551-63
- [41] Benedict S, Singh M, Naik T R R, Shivashankar S A and Bhat N 2018 Microwave-synthesized NiO as a highly sensitive and selective room-temperature NO₂ sensor ECS J. Solid State Sci. Technol. 7 Q3143–7
- [42] Halfaya Y et al 2016 Investigation of the performance of HEMT-based NO, NO₂ and NH₃ exhaust gas sensors for automotive antipollution systems Sensors 16 273

- [43] Kumar A et al 2018 Modeling of gate bias controlled NO₂ response of the PCDTBT based organic field effect transistor Chem. Phys. Lett. 698 7–10
- [44] Huang W et al 2017 UV-Ozone interfacial modification in organic transistors for high-sensitivity NO₂ detection Adv. Mater. 29 1701706
- [45] Wang Z et al 2018 Rational synthesis of molybdenum disulfide nanoparticles decorated reduced graphene oxide hybrids and their application for high-performance NO₂ sensing Sens. Actuators B 260 508–18
- [46] Wang J et al 2016 Hierarchical ZnO nanosheet-nanorod architectures for fabrication of Poly(3-hexylthiophene)/ZnO hybrid NO₂ sensor ACS Appl. Mater. Interfaces 8 8600–7
- [47] Henderson M A, Epling W S, Perkins C L, Peden C H F and Diebold U 1999 Interaction of molecular oxygen with the vacuum-Annealed TiO₂ (110) surface: molecular and dissociative channels J. Phys. Chem. B 103 5328–37
- [48] Lee F K, Andreatta G and Benattar J-J 2007 Role of water adsorption in photoinduced superhydrophilicity on TiO₂ thin films Appl. Phys. Lett. 90 181928